Circulations Associated with a Mature-to-Decaying Midlatitude Mesoscale Convective System. Part I: Surface Features—Heat Bursts and Mesolow Development

RICHARD H. JOHNSON, SUE CHEN* AND JAMES J. TOTH**

Department of Atmospheric Science, Colorado State University, Fort Collins, Colorado

(Manuscript received 25 August 1988, in final form 17 November 1988)

ABSTRACT

This study examines surface features associated with a mature-to-dissipating midlatitude mesoscale convective system that occurred on 23–24 June 1985 during the Oklahoma–Kansas Preliminary Regional Experiment for STORM–Central. The primary data sources include a 400 × 500 km surface mesonetwork on a 50 km grid, rawinsonde observations from 12 supplementary sites in Kansas and Oklahoma and radar measurements from conventional as well as dual-Doppler networks.

The mesoscale convective system under investigation developed in an environment with weak vertical shear and had a lifetime of 9–12 h. It consisted in its mature stage of a southward-moving arc-shaped line of deep convective cells with a trailing stratiform precipitation region to the north. Thirty-three percent of the surface rain in the portion of the mesonetwork experiencing storm passage was from the stratiform region. An intense mesoscale downdraft developed beneath the stratiform cloud with a strong mesohigh at the surface. A wake low was positioned just to the rear of the trailing stratiform region. Local "heat bursts" were observed within the wake low. These phenomena are tentatively attributed to downbursts (which develop in a nearly dry-adiabatic environment created by the mesoscale downdraft) that penetrate a shallow, stable layer near the ground.

During the final dissipation of the stratiform precipitation (in a matter of 2 h), the surface mesohigh transformed into a mesolow. Observations suggest that at least part of this transformation process can be explained as a collapsing cold pool or spreading density current. This mechanism may also have contributed to the observed development or intensification of a midlevel mesovortex as the storm dissipated. Following the decay of the mesoscale convective system during the nighttime hours, new deep convection broke out in the region of the remnant midlevel circulation the next morning.

1. Introduction

A prominent characteristic of deep convection in the tropics and summertime midlatitudes is the tendency for convective elements to organize to form larger scale or mesoscale cloud systems (e.g., Houze and Hobbs 1982). The horizontal dimensions and lifetimes of such systems are sufficiently great that the earth's rotation can significantly affect the storm-generated circulations. In the upper troposphere, pronounced anticyclonic circulations forced by the convective heating aloft have been observed and modeled (e.g., Fritsch and Chappell 1980; Fritsch and Maddox 1981a,b; Maddox et al. 1981).

Receiving less attention, until recently, are cyclonic circulations which have been observed to develop in the midtroposphere within the mesoscale convective systems (Houze 1977; Leary 1979; Ogura and Liou 1980; Johnston 1982; Bosart and Sanders 1981; Gamache and Houze 1982; Maddox 1983; Smull and Houze 1985; Leary and Rappaport 1987; Zhang and Fritsch 1987 and 1988; Menard and Fritsch 1988), along with their associated surface pressure features. Leary and Rappaport (1987) clearly show the development of a midtropospheric cyclonic circulation or mesovortex, accompanied by curved rainbands, within the trailing stratiform region of a mesoscale convective system over Texas. These midlevel circulations have been often observed to last for several days (Johnston 1982; Wetzel et al. 1983; Zhang and Fritsch 1988; Menard and Fritsch 1988), have in some instances exhibited a warm-core structure, and may even be related to the development of some tropical cyclones (Velasco and Fritsch 1987).

In this paper we present observations relating to the development of a midtropospheric cyclonic circulation during the decay of a nocturnally generated, midlatitude mesoscale convective system (hereafter referred to as an MCS). The system studied occurred on 23–24 June 1985, over the central United States during the Oklahoma–Kansas Preliminary Regional Experi-

* Current affiliation: National Center for Atmospheric Research, Boulder, CO 80307.

** Current affiliation: Naval Environmental Prediction Research Facility, Monterey, CA 93943-5006.

Corresponding author address: Dr. Richard H. Johnson, Dept. of Atmospheric Science, Colorado State University, Fort Collins, Colorado 80523.

© 1989 American Meteorological Society

ment for STORM-Central (OK PRE-STORM). In this study (Part 1) we focus on the surface features associated with the circulation spin-up, features which have heretofore been difficult to document due to the sparsity of surface observations normally available for these events. Several aspects of this phenomenon not treated before will be investigated here:

(i) The relationship of surface mesolow development to the radar-determined cloud and precipitation structure of a mature-to-decaying MCS that contains a developing mesovortex;

(ii) The characteristics of "heat bursts" (Johnson 1983) which accompanied this system, and relationship of these phenomena to strong downdrafts on the mesoscale; and

(iii) The life cycle of a surface mesolow associated with the rapidly decaying stratiform cloud system within the MCS, including its relationship to the regeneration of deep convection the next day.

Yet another aspect of this case, mesoscale circulations associated with the MCS treated here and another adjacent to it (producing an interaction which complicated forecasts of new convective development on this day), has been recently reported by Stensrud and Maddox (1988). In Part II we present the vertical structure of the circulation and Doppler radar and rawinsonde-derived vertical motions for the system.

2. Data and analysis procedures

a. Surface mesonetwork and upper air observations

The surface and upper air networks employed in OK PRE-STORM are discussed and illustrated in Cunning (1986) and Johnson and Hamilton (1988). In order to obtain meaningful representations of the surface pressure field, adjustments have been made to the reported surface pressures using the procedures described in Johnson and Hamilton (1988). These procedures include correction for instrument error based on calibration records and comparison with surrounding National Weather Service stations. The pressure corrections used for the NCAR PAM (Portable Automated Mesonetwork) stations are identical to those reported in Table A1 of Johnson and Hamilton (1988), while those from the NSSL (National Severe Storms Laboratory) SAM (Surface Automated Mesonetwork) stations are similar to those in Table A1. In the treatment of sounding data, accounting has been made for balloon drift and variable release times. Data from the 50 MHz wind profiling system at Liberal, Kansas (Augustine and Zipser 1987) have also been used in the analyses.

b. Radar and satellite data

Radar data used in this study are from the NCAR (National Center for Atmospheric Research) CP-3 and CP-4 5 cm wavelength Doppler radars and several digitized NWS (National Weather Service) WSR-57 10 cm radars. Details of the radar characteristics and scanning strategies of CP-3 and CP-4 are provided in Rutledge et al. (1988). Satellite data are from GOES West, a United States geostationary satellite which was situated at 105°W during the experiment.

3. Synoptic setting and satellite and radar overview

This case is an outstanding example of upscale development of convection. Convective cells first formed during the afternoon or around 1900 (all times UTC) 23 June along a dryline in western Kansas ahead of an approaching cold front (see 2100 surface analysis in Fig. 1), with additional growth along a line extending northeastward across southern Nebraska and southwestward to northeastern New Mexico. A visible satellite image of the development by 2130 is shown in Fig. 2a. Cell movement along the line was east to east-southeast in northern Kansas and southern Nebraska whereas movement in central and southern Kansas was to the south.

Between 2130 on the 23rd and 0400 on the 24th the discontinuous line of convection across Kansas and

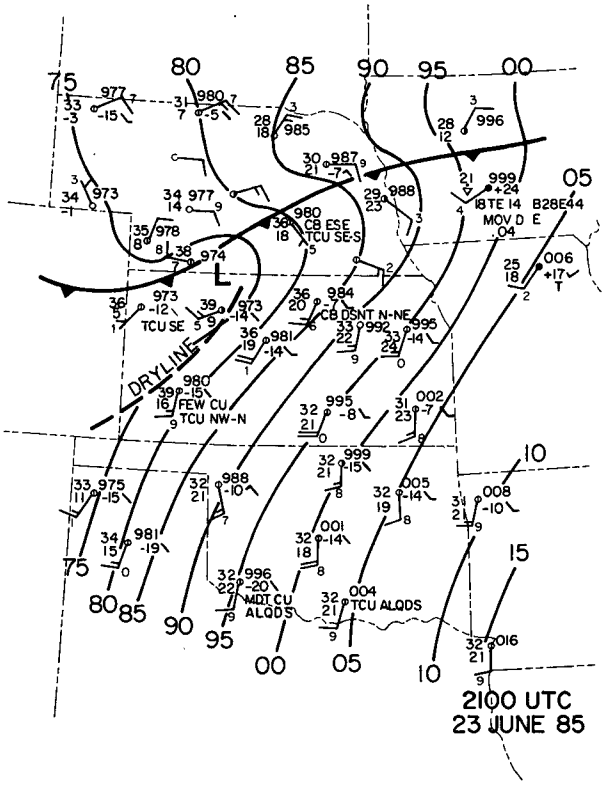

FIG. 1. Surface analysis for 2100 UTC, 23 June 1985. Isobars are for altimeter settings, adjusted to 400 m using a modification of the procedure by Sangster (1987), in units of in Hg (e.g., 90 = 29.90 in Hg). For wind speed, one full barb = 5 m s^{-1}, one half barb = 2.5 m s^{-1} (similarly in subsequent figures).

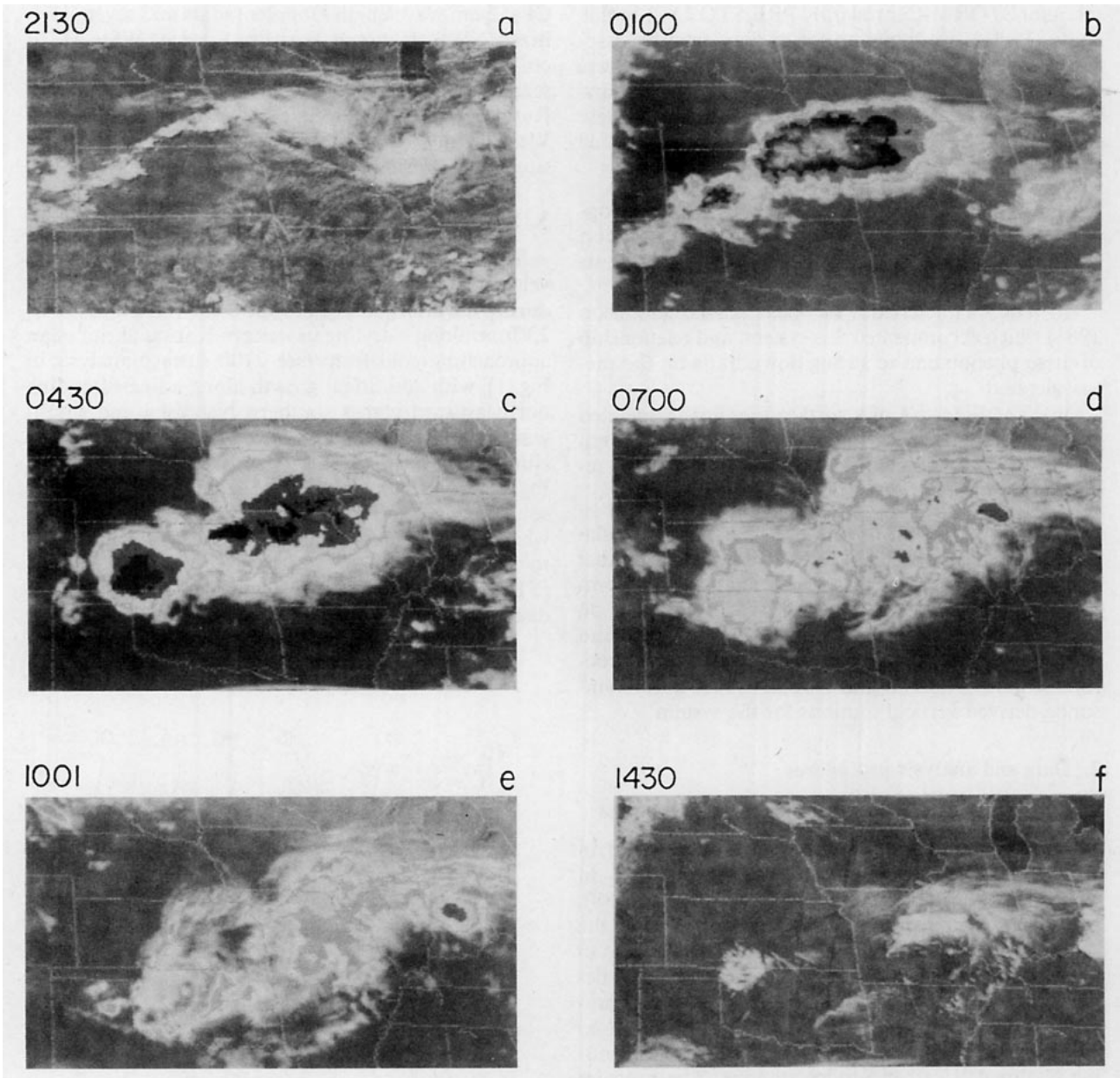

FIG. 2. Satellite pictures for 23–24 June 1985 at (a) 2130, (b) 0100, (c) 0400, (d) 0700, (e) 1001 and (f) 1430 UTC.

Nebraska consolidated into two primary convective systems (see infrared images in Figs. 2b and 2c). Although the eastern MCS was the larger of the two and was investigated by research aircraft, only the western storm traversed the intensive PRE-STORM network and provides the focus of this study. Three hours later, at 0700, both systems weakened considerably as evidenced by the reduction in the area of cold cloud tops (Fig. 2d). Further weakening occurs over the next 3 h (Fig. 2e) and there is a slight hint of cyclonically-curved bands in the remnant cloud fields of both MCSs. These cloud patterns somewhat resemble the "mesovorticity centers" identified in satellite images by Johnston (1982). Following sunrise on the 24th, some new convection broke out on the Kansas–Oklahoma border and over eastern Missouri (Fig. 2f), presumably associated with the remnant circulation systems.

Although the primary emphasis in this paper (Part I) is on surface features, several upper air analyses will be presented so that the surface data can be put into the context of the upper-level vortex. Part II will provide a detailed analysis of the upper level structure of the convective system. The 500 mb analysis in Fig. 3 shows a weak short-wave trough passing just to the

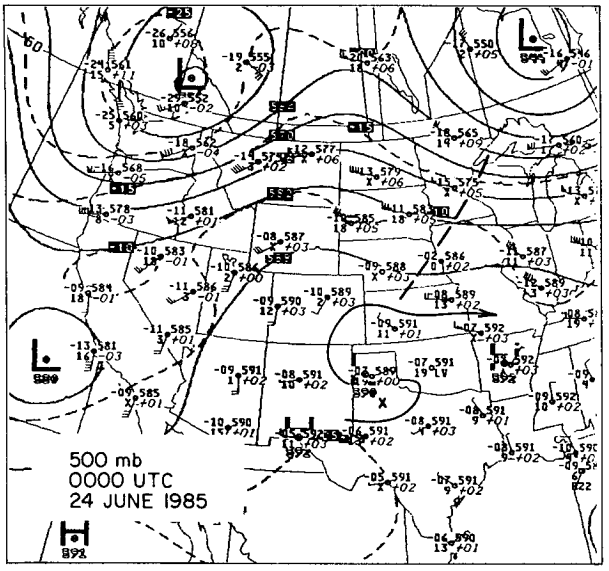

FIG. 3. 500 mb analysis, 0000 UTC, 24 June 1985. Streamline is added to represent the flow field over the area of study. X marks position of absolute vorticity center on National Meteorological Center LFM (Limited-area Fine-mesh model) initial analyses.

north of the Kansas–Oklahoma region at 0000 on the 24th. A weak cyclonic circulation also exists over northern Texas. By 1200 the next morning (Fig. 4) there is evidence, based on the conventional synoptic-scale sounding data, of two circulation centers or positive relative vorticity maxima at 500 mb, one associated with each of the MCSs in Fig. 2.

A closer view of the 500 mb circulation over Kansas and Oklahoma is shown in Figs. 5a and 5b at 0515 and 0900. In Fig. 5a, sounding data from PRE-STORM supplemental and profiler sites have been composited from 0430 to 0600 assuming a storm movement toward 170° at 10 m s^{-1}. This storm motion is based on radar-tracking the stratiform region over a 3-h period from 0500 to 0800. The analysis at 0900 (Fig. 5b) is primarily based on 0900 data, although observations from as early as 0600 and as late as 1200 (indicated by dashed wind barbs) are included in the figure after appropriate displacement for storm motion. The latter observations are given less weight in the analysis since the storm was clearly not steady over the 6-h period. In particular, there appeared to be a considerable slowdown in the southward motion after 0900.

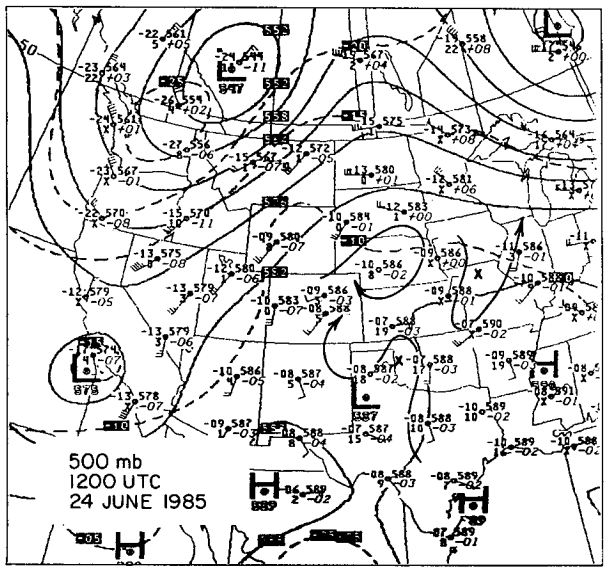

FIG. 4. As in Fig. 3, except at 1200 UTC.

At 0515 (Fig. 5a) there appears to be a trough line oriented NE–SW over Kansas with the axis of the trough positioned somewhere in the trailing stratiform regions of both systems. Dual-Doppler radar analysis of the western MCS 2 h later (0723), to be presented in Part II, shows strong cyclonic curvature in the wind field along the northern periphery of the stratiform area, whose northern boundary is itself cyclonically curved. This information is used in placing the trough axis in Fig. 5a, although it is admitted that a definitive analysis cannot be drawn. By 0900 (Fig. 5b) the formation of a separate vortex over southern Kansas appears to be occurring, which eventually ends up as a vorticity center over northwestern Oklahoma (Fig. 4). While a sharp trough (possibly containing a closed circulation) is apparent at 1200 (Fig. 4), supplemental sounding data do not exist to give its detailed structure. WSR-57 radar data from Wichita, Kansas, show that by 0900, most of the precipitation had dissipated, with only weak echoes remaining near WWR. Dual-Doppler radar data from CP-3 and CP-4 at 0827, when somewhat more precipitation was present, have been added to the 0900 composite analysis (following an appropriate displacement) and have been used to pinpoint the trough axis.[1] A portion of the vortex associated with the eastern MCS over Missouri is also evident at this time.

Figure 5b is a slight improvement of our earlier analysis for this case published in Zhang and Fritsch (1987; their Fig. 12) and includes Profiler and dual-Doppler radar data. It shows that when viewed in a broad sense, the circulation has a warm core, but the warm air appears to be on the northern edge of the developing vortex with relatively cool air in the remnant stratiform area to the southwest. The dual-Doppler radar data (Part II) show strong subsidence in the midtroposphere along the northern edge of the precipitation area and this information is used to place the warmest air just north of the trough axis. The analysis is not conclusive, however, and it may be that the warm core extends farther south. As will be shown later, very

[1] The analysis dramatically illustrates the relatively small portion of this developing mesovortex sampled by the single dual-Doppler array in Kansas.

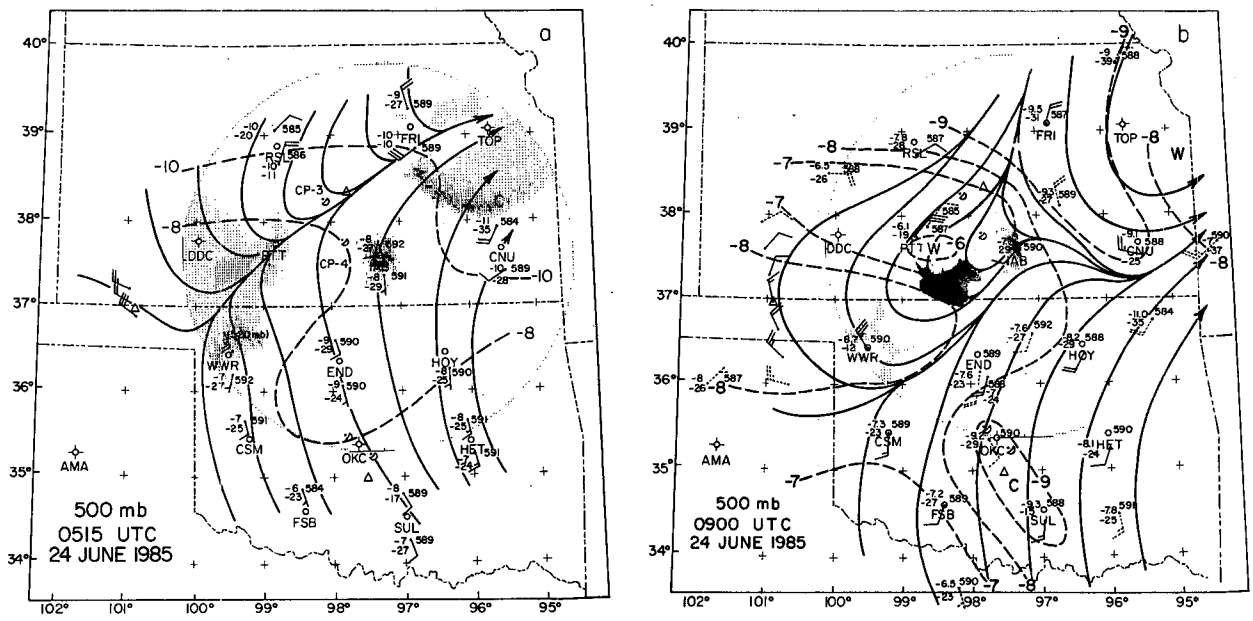

FIG. 5. Composite regional 500 mb analyses on 24 June 1985 at (a) 0515 and (b) 0900 UTC. Analysis at 0900 UTC is based primarily on 0900 UTC observations. Data 3 h earlier and later than 0900 are indicated by dashed wind barbs. Stippling represents reflectivity at thresholds of 18, 30, 40, 45 and 50 dBZ. Shading near center of (b) represents region of dual-Doppler winds at 0827 UTC displaced to appropriate 0900 UTC position. Small arrows in this region indicate Doppler-derived wind directions. Dashed lines are isotherms (°C).

warm air exists in the lower troposphere beneath the remnant stratiform cloud system (near WWR), and, in fact, a strong surface mesolow also exists at this time on the Oklahoma–Kansas border north of WWR (Fig. 12d later).

Digitized radar data from the WSR-57 radars at Wichita, Kansas, are used in Fig. 6 to depict the precipitation structure of the MCS during its mature to dissipating stages. Similar data from the site at Goodland, Kansas, are available, but are severely contaminated by anomalous propagation and are not used. Two storm systems are evident at 0205 (Fig. 6a; corresponding to the two primary cloud systems in Figs. 2a and 2b), which are characterized by deep convective cells on their southern periphery with a stratiform area to the north. The systems moved to the south at about 10 m s^{-1}, retaining a similar structure of a leading convective line and a trailing stratiform region (Fig. 6b). By 0601 (Fig. 6c), the leading convective line in the western system has nearly completely dissipated, although the stratiform precipitation has expanded and intensified somewhat. From 0700 to 0900 (Figs. 6d–f) the stratiform areas diminished, first slowly and then more rapidly, such that by 0900 nearly all stratiform precipitation ended.

4. Precipitation analysis

The radar depiction of a portion of the MCS life cycle in Fig. 6 indicates that both convective and stratiform precipitation are present. Time series of rainfall at a number of the mesonet stations experiencing passage of the system reveal the separate convective line and trailing stratiform precipitation components. An example is shown in Fig. 7 for P26 (PAM station 26 in southwestern Kansas; position indicated later in Fig. 9a). The rainfall record for this station shows heavy rain beginning just before 0400 and lasting only 25 min, then an approximate 1 h period of little to no rain, followed by a 1.5 h period of light stratiform rain. In radar analyses, the intervening period of little to no rain is referred to as the transition zone or reflectivity trough by Smull and Houze (1987a) and Chong et al. (1987). It can be explained by the rearward transport of hydrometeors (snow and ice) from high levels in the leading convective line in such a way that the zone of maximum fallout as stratiform rain is well behind the line (Smull and Houze 1985; Rutledge and Houze 1987). The pressure trace shows a pronounced mesohigh straddling the entire period of rainfall, with the highest pressure occurring during the stratiform rain. Normally, during a squall line passage, the peak pressure occurs with the convective rain (Fujita 1955). Our case is somewhat different and, as will be discussed later, this intense mesohigh in the stratiform rain area and its subsequent rapid collapse may shed some light on mechanisms for the rapid development of a pronounced surface low and the intensification of a midlevel mesovortex in this case.

By examining rainfall traces for all mesonet stations, a determination can be made of the relative contributions to the total rain by convective and stratiform

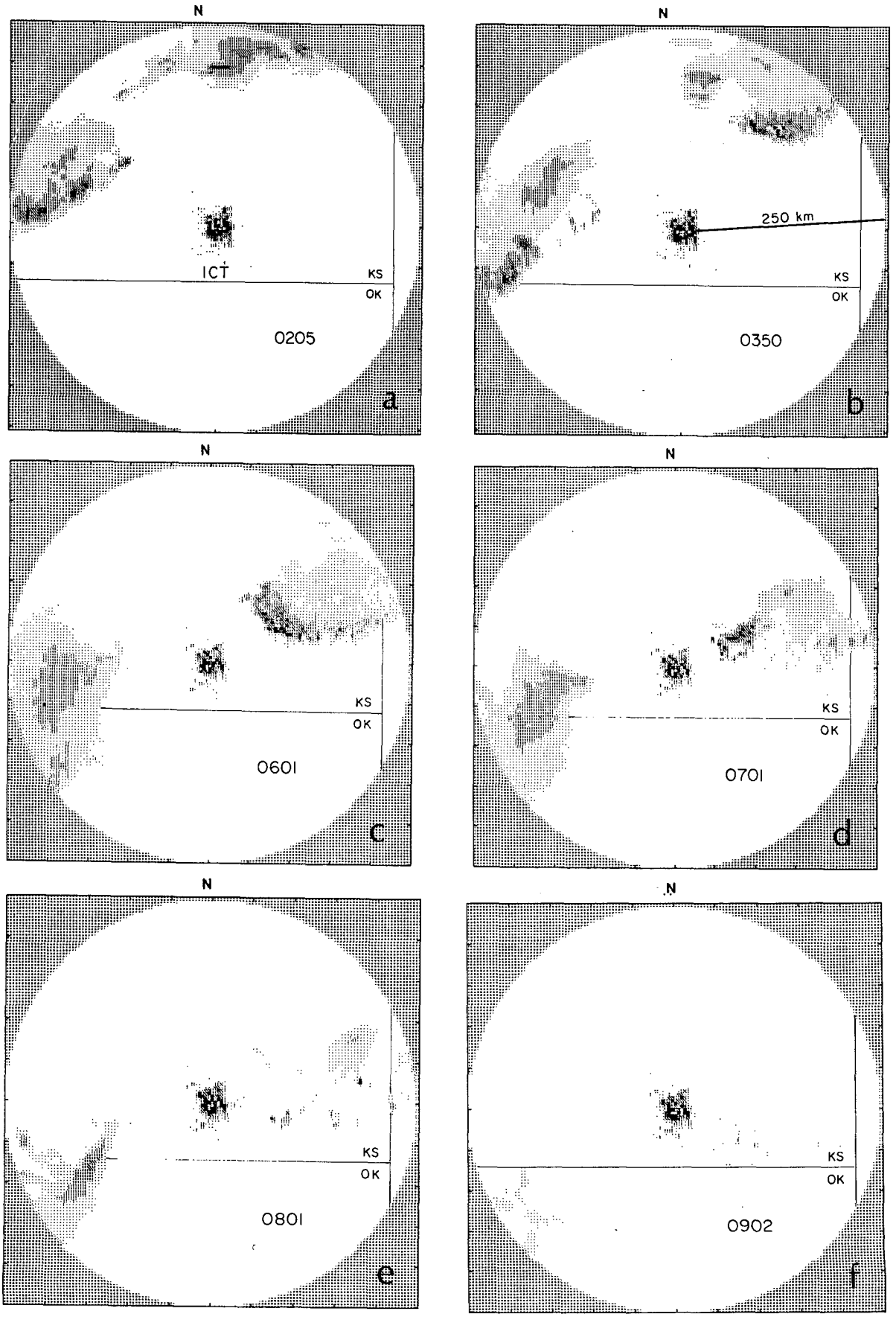

FIG. 6. Low-level radar reflectivity from Wichita, Kansas, on 24 June 1985 at 0205, 0350, 0601, 0701, 0801 and 0902 UTC. Reflectivity thresholds are 18, 30, 40, 45 and 50 dBZ.

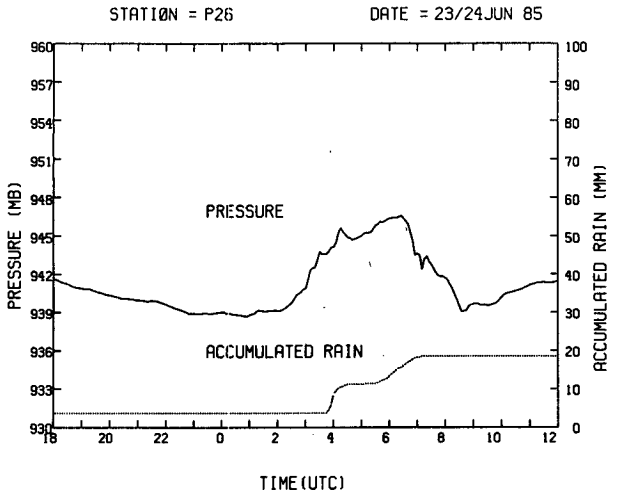

FIG. 7. Time series of pressure (mb) and accumulated rain (mm) at PAM station 26 (see Fig. 9a later) in southwestern Kansas from 1800 UTC 23 June to 1200 UTC 24 June 1985.

components. Such computations were made for the 10–11 June PRE-STORM squall line case by Johnson and Hamilton (1988). In that study and this one it is assumed that when the 5-min rainfall rate exceeds 0.5 mm per 5 min, it is convective line rainfall, and when it decreases to a rate less than or equal to this value (even if it later increases), it is stratiform rain. The results of this analysis are shown in Fig. 8. The total convective line rain amounts are greatest, exceeding 20 mm at two stations, on the western fringe of the mesonetwork. On the other hand, the stratiform rain maximum occurs in the interior of the mesonetwork, although the peak totals are somewhat less (about 8 mm). The eastward displacement of the stratiform rain maximum suggests that much of this light precipitation is a consequence of advection of hydrometeors from deep convective cells to the west by westerly flow (relative to the storm) aloft. Some of the stratiform rainfall may also be a result of in situ generation of new condensate by a mesoscale updraft and vapor deposition onto existing ice particles in the region of mesoscale ascent (Brown 1979; Ogura and Liou 1980; Gamache and Houze 1982; Smull and Houze 1987a; Rutledge and Houze 1987).

The fraction of the total rain due to the stratiform component is also shown in Fig. 8. On the eastern fringe of the rain area 100% of the rain is stratiform with decreasing percentages to the west, as inferred from the first two panels of Fig. 8 and explained earlier by the westerly relative flow aloft. The region of greatest stratiform rain amount roughly coincides with the areas of maximum rainfall duration (last panel in Fig. 8), as expected. Important to future discussion is the co-location of the greatest stratiform rainfall area with subsequent surface mesolow formation and midtroposphere mesovortex development.

The average stratiform rain fraction based on the accumulated rainfall from all stations experiencing the passage of this system is 33%. This percentage is very close to the 29% stratiform rain fraction determined for the 10–11 June 1985 squall line, a much more extensive (800 km long) midlatitude convective system. It is notable that similar results are obtained for convective lines having very different along-line dimensions, suggesting that the physical processes producing trailing stratiform rainfall are likely independent of the

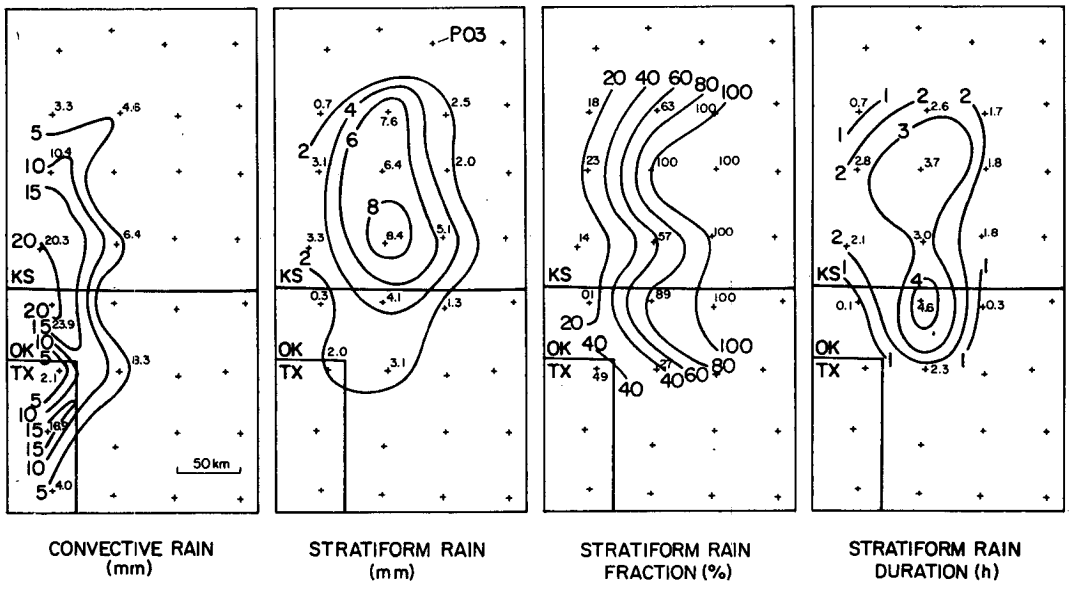

FIG. 8. Convective rain, stratiform rain, stratiform rain fraction and stratiform rain duration for 23–24 June 1985 mesoscale convective system.

horizontal scale of the overall system (as also suggested by the 2-D modeling results of Rutledge and Houze 1987). The stratiform rain fraction is also within the range of the 30 to 50% fractions determined from radar data for tropical squall lines and mesoscale convective systems by Houze (1977); Cheng and Houze (1979); Houze and Rappaport (1984); Leary (1984); Churchill and Houze (1984) and Wei and Houze (1987).

5. Surface observations

a. MCS mature stage and "heat burst" occurrence

The effects of the developing convection in western Kansas first appeared in the surface mesonetwork around 0000. By 0200 the convective line and trailing stratiform region had entered the northwest portion of the PAM network (Fig. 9a). At this time a strong surface mesohigh is centered just to the rear of the leading convective cells with a wake low near the back edge of the stratiform region (although the location of the low center cannot be determined). The positioning of these features is consistent with the analyses of the surface perturbation pressure field for squall lines presented by Fujita (1955), Pedgley (1962) and Johnson and Hamilton (1988). Johnson and Hamilton have presented observations to indicate that the wake low is a surface manifestation of the *rear-inflow jet*, a system-relative rear-to-front flow that descends toward the convective line (Smull and Houze 1987b). A weak presquall mesolow also appears ahead of the surface gust front. Effects of the eastern MCS (indicated by radar in Fig. 9a) are not present in the mesonetwork at this time.

By 0400 (Fig. 9b) the gust front from the eastern MCS has entered the northeast portion of the mesonetwork and the gust front and mesohigh associated with the western MCS have entered Oklahoma, having moved south at 10 m s^{-1}. The *northern edge* of the trailing stratiform region moved south much more slowly (at 5 m s^{-1}) during this period, reflecting an expansion of the stratiform area. The wake low still appears to be just outside the network; however, a much stronger pressure gradient (locally reaching 1 mb/5 km) is now observed between the mesohigh and the wake low.

A striking feature of the flow at 0200 is the presence of hot, dry air or a "heat burst" (Johnson 1983) at P03 (see Fig. 9a, top row). The 5-min average temperature and dewpoint at this time are 34° and 2°C, respectively, indicating a relative humidity of 12%! A time series of temperature and dewpoint at this station (Fig. 10, top-center panel) dramatically illustrates these heat bursts. Between 2345 and 0400 there are five primary temperature spikes, having amplitudes of 2° to 4°C. No-

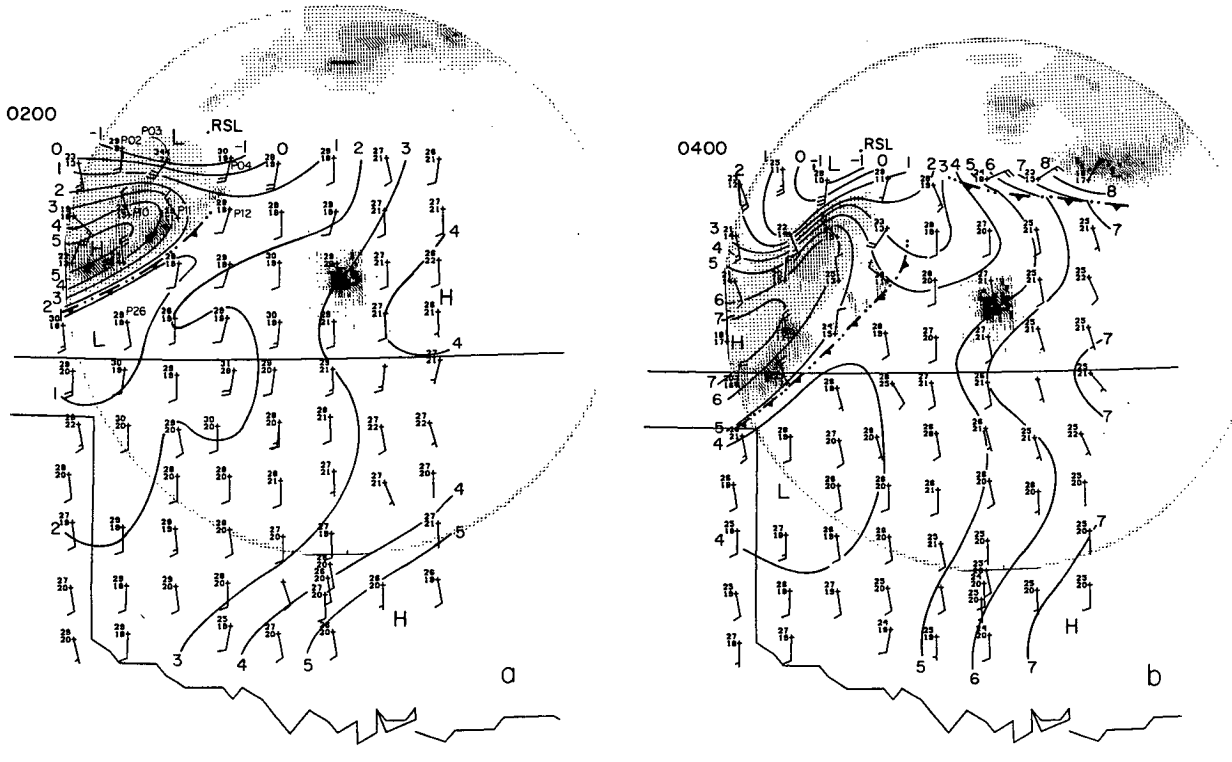

FIG. 9. Surface mesonetwork analysis at (a) 0200 and (b) 0400 UTC on 24 June 1985. Contours represent pressure adjusted to 518 m (approximate height of the average station elevation in the region) given as departures in mb from 950 mb (e.g., +1 = 951 mb). Temperature and dewpoint are in deg C. Reflectivity thresholds are 18, 30, 40, 45 and 50 dBZ. Dashed, double-dotted line indicates gust front position. Identifiers are given for stations 2, 3, 4, 10, 11, 12 and 26.

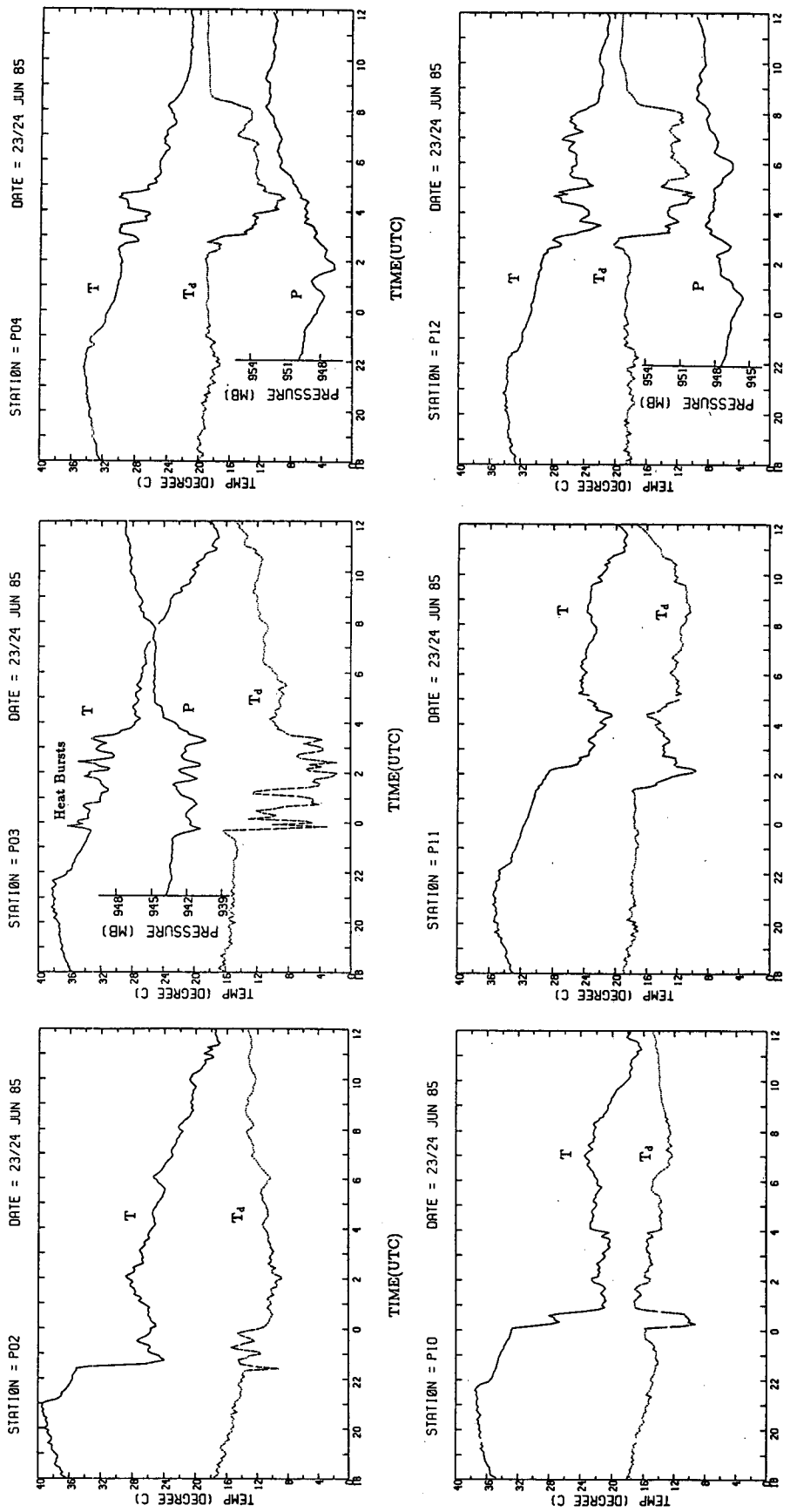

FIG. 10. Time series of temperature, dewpoint temperature and pressure at PAM stations 2, 3, 4, 10, 11 and 12 from 1800 UTC 23 June 1985 to 1200 UTC 24 June 1985. Positions of stations are indicated in Fig. 9a. Heat bursts are most prominent at station 3.

tably, a jump to 35°C (or 95°F) occurred near sunset (0230). P04 and P12 also exhibit heat burst activity (Fig. 10), although the peak temperatures are not as high (spacing between individual stations is ~50 km). At P02, P10 and P11, on the other hand, heat bursts are not so evident, with the temperature trace characterized primarily by a sharp cooling with the arrival of the leading convective line followed by only minor temperature recovery.

During the period of the heat bursts at P03 the wind was generally south-southwesterly between 10 and 15 m s^{-1}. However, at the time of each burst there was a wind shift to a more westerly direction and a reduction in speed, with the greatest changes occurring at the time of the strongest heat burst near 0230 (windshift to 250°, speed drop to 4 m s^{-1}). No rain fell at P03 (nor adjacent stations P02, P04 and P12) throughout the entire storm episode, although mostly light rain fell to the south at P10 (12.2 mm between 0045 and 0355) and P11 (2.5 mm between 0305 and 0440) during the heat burst period (see also 2nd and 4th panels of Fig. 8). From an examination of data from the NCAR CP-3 Doppler radar (117°, 105 km from P03) for this time period, it is apparent that while P03 was situated just to the north of the region of surface stratiform precipitation during the heat burst period, it was in a region having deep stratiform cloud overhead. The CP-3 radar reflectivity data indicates a stratiform cloud layer at 0232 extending from approximately 4 to 11 km above P03. A wake low also persisted in the P03 region during this time (Figs. 9a, b and Fig. 10).

At the time of each heat burst there is generally a corresponding sharp drop in the dewpoint with fluctuations as large as 10°C occurring at P03. A strong negative correlation is observed between temperature and dewpoint fluctuations at P03 and P12 during the burst periods, which is indicative of repeated penetrations of warm, dry air from aloft. There is also a significant decrease in the average dewpoint temperature throughout the entire 4 to 5 h periods of heat burst activity at P03, P04 and P12. Virtually all of the earlier studies of heat bursts have also indicated that they are very dry (e.g., Johnson 1983).

The duration of bursts ranges from 15 to 70 min, averaging 39 min, with the periods between them being quite irregular. This average duration is somewhat shorter than the order of 1 to 2 h bursts reported by Williams (1963) and Johnson (1983); however, Johnson (1983) indicates that shorter events have been documented in her review of previous studies on this subject. The durations in our case are quite similar, however, to those reported by Bedard and LeFebvre (1986) for dry downbursts[2] occurring near Denver's Stapleton Airport during the 1982 JAWS (Joint Airport Weather Studies) Project. The average duration of the 20 macrobursts[3] they observed was 53 min.

The similarity in duration (and other properties to be discussed) between heat bursts and downbursts suggests that the mechanisms for the two may be similar. In fact, we believe there is evidence from our study that supports the hypothesis advanced by Johnson (1983) that heat bursts are essentially downbursts impacting on a stable layer near the ground. The heat burst occurs when air in the downburst overshoots its equilibrium point and becomes warmer than its surroundings upon reaching the surface. We present observations in this subsection that tend to support this idea.[4] However, we do not have direct measurements of the downbursts themselves (not resolvable at the far range of the NCAR CP-3 Doppler radar, though deep stratiform cloud aloft was detected), so that our conclusions should be regarded as largely inferential.

A sounding taken in the vicinity of these heat bursts [from RSL (Russell, Kansas, see Fig. 9) at 0440], is illustrated in Fig. 11. Except for a stable layer near the ground, a deep, nearly dry-adiabatic layer exists below 500 mb with very dry conditions in the lower troposphere. This sounding resembles very closely the heat burst soundings presented in Fig. 10 of Johnson (1983). There it is remarked that such soundings are very similar to dry microburst soundings over the High Plains (e.g., Brown et al. 1982; Wakimoto 1985). They also resemble the "onion" soundings in and to the rear of the trailing stratiform regions of tropical (Zipser 1977; Houze 1977) and midlatitude (Ogura and Liou 1980; Leary and Rappaport 1987) MCSs, except that in the heat burst cases there is a much shallower layer of cool, moist air near the ground. Williams (1963) examined numerous cases of lower tropospheric warming and drying to the rear of squall lines, but noted that instances where the warm, dry air penetrated all the way to the surface were rare.

Johnson (1983) suggests that because heat bursts occur in environments similar to those for dry microbursts, the mechanism for their origin may be similar. Specifically, heat bursts may develop when precipita-

[2] Fujita and Wakimoto (1981) define a downburst as a strong downdraft which induces an outburst of damaging winds on or near the ground.

[3] A macroburst is a downburst whose surface outburst horizontal dimensions exceed 4 km; if they are less than or equal to 4 km, the downburst is called a microburst (Fujita 1985).

[4] Alternative explanations for heat bursts might argue that they are a manifestation of wave phenomena (e.g., gravity waves) or some other dynamical mechanism that can induce strong sinking motion. The relatively long duration and localized nature of the heat bursts suggests that a wave phenomenon is unlikely. Dynamically forced subsidence may, on the other hand, play some role, although the role is at this time difficult to define specifically. The existence of a wake low in the vicinity of the heat bursts at the trailing edge of the stratiform region suggests strong subsidence is occurring in this area (similar to that observed in the 10–11 June squall line studied by Johnson and Hamilton 1988). Dual-Doppler radar analyses somewhat later (0723) confirm the existence of a system-relative rear inflow entering the storm and descending at the back edge of the stratiform region (Part II).

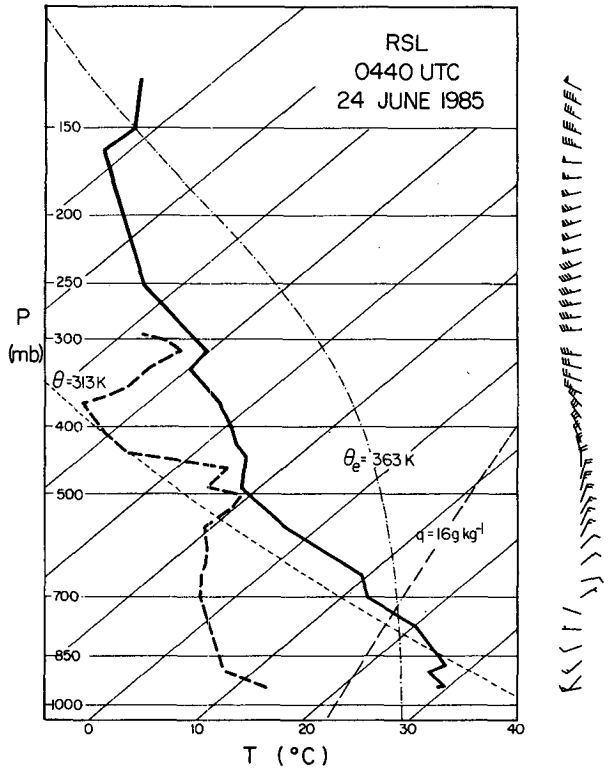

FIG. 11. Skew-T plot for Russell, Kansas, at 0440 UTC 24 June 1985.

tion is introduced aloft (in our case from the trailing stratiform cloud) and is evaporated in a nearly dry-adiabatic environment. Observations of precipitation aloft at P03 are evident from the 0205 Wichita radar display (Fig. 9a), the NCAR Doppler radars (not shown) and are suggested, though not confirmed, by surface observations from RSL (Table 1). The observations at RSL of RWU SW and CB MAM SW (Table 1) are not inconsistent with the existence of showers generating downbursts near P03 (P03 is 40 km southwest of RSL).

By the time the air reaches low levels, a strong downdraft may develop. If this downdraft air penetrates a shallow stable layer near the ground (Fig. 11), a layer in our case which is attributable to outflows from the leading convective line (as described by Zipser 1977), it will rapidly lose its negative buoyancy. However, if it has enough downward momentum to reach the surface, pronounced localized warm anomalies may result. Bedard and LeFebvre (1986) give a condition for penetration of downburst air to the surface in terms of a Froude number, Fr:

$$\mathrm{Fr} = W \Big/ \left(\frac{\Delta T}{T} gh\right)^{1/2}, \qquad (1)$$

where h is the depth of the ground-based inversion, W is the downflow speed of the microburst, ΔT is the temperature difference between stable surface air and microburst/ambient air and T is the local mean temperature. For Fr > 1, microbursts should penetrate to the surface whereas for Fr < 1, midair microbursts (Fujita 1985) should result. The sounding from Russell (Fig. 11) indicates that the 34°C at station 3 can be explained by adiabatic descent of air from 900 mb. The 2°C dewpoint requires air from somewhat higher (near 800 mb). Considering that 0440 RSL sounding was taken approximately 2 h after the last 2°C dewpoint heat burst and was located ~40 km northeast of the heat burst site, it is probably unwise to precisely relate conditions at P03 to the RSL sounding. Nevertheless, if we use this sounding as a general indicator of the strength and depth of the surface-based inversion, wherein we assume ΔT = 2 to 4 K and h = 500 m, then penetration to the surface can be expected for downdraft speed W of 6 to 8 m s^{-1}. Measurements are not available to confirm these estimates; however, Johnson (1983) reports downdrafts of this magnitude determined by tower data for the downburst cases she studied.

Fujita (1985) and Bedard and LeFebvre (1986) have observed that some dry microbursts, e.g., those observed during JAWS, are accompanied by a cooling and some by a warming, although there appears to be a preference for cooling along with a pressure rise at the surface. Cooling at the surface should be expected for the typical dry microburst sounding (Wakimoto 1985) where the dry-adiabatic lapse rate extends all the way to the surface or to the top of a superadiabatic layer near the surface.

Williams (1963) and Johnson (1983) indicate surface pressure falls of 2–4 mb during the heat bursts they

TABLE 1. Surface observations from Russell, KS, 23–24 June 1985.

Time (UTC)	Sky cover	Weather	Remarks
2150	40 SCT 250 SCT		TCU N
2250	E50 BKN 250 BKN		CB W-N TCU W-N LN BLDG CU SW-N RWU SW-W
2350	E50 BKN 250 BKN		CB SW DRK SW RWU SW TCU SW
0050	E50 BKN 250 BKN		DRK SW CB SW-N RWU SW CB MAM W
0115	E50 BKN 250 BKN	T	TB 15 T SW MOVT UNK RWU SW DRK SW LTGCC SW PK WND 1944 15
0150	E50 BKN 250 BKN		TE 40 MOVG SW RWU SE-S DRK SE-S
0250	E50 BKN 250 BKN		FQT LTGICCG S

studied. Similar pressure fluctuations occurred at P03 with each of the five bursts accompanied by a pressure fall, averaging about 2 mb (Fig. 10). However, at P04 and P12 the pressure fluctuations occurring during heat bursts were minor and not well-correlated with the bursts (Fig. 10). Bedard and LeFebvre (1986) indicate that a variety of surface pressure responses can occur when a downburst impacts on a stable layer near the ground. Pressure falls can be attributed to the lateral displacement of cool, stable air near the ground by downdrafts. In the case of heat bursts, falls can probably also occur as a hydrostatic consequence of intense local warming in the lower troposphere. For example, assuming an average 2°C warming (Fig. 10) over a 1 km layer above the ground, a hydrostatic surface pressure fall of 0.7 mb should be realized for the strongest bursts at P03. The observed falls up to 2 mb suggest that the displacement of cooler air is also an important factor in this case. When a station is directly under an impacting downburst, it can alternatively experience a pressure rise as the stagnation pressure builds up (Fujita 1985; Bedard and LeFebvre 1986). The contribution of this effect to surface pressure change is difficult to estimate in our case due to lack of appropriate data.

Fujita (1985) has hypothesized a downburst mechanism associated with anvil clouds that we adopt here and combine with the concepts introduced by Zipser (1977), Johnson (1983) and Bedard and LeFebvre (1986) to propose as an explanation for the heat burst events. Fujita notes that microbursts have been observed descending beneath virga from anvil clouds in their postmature stages. When occurring in stratiform cloud systems to the rear of squall lines, these downbursts often descend in a nearly dry-adiabatic environment above a deep stable layer near the ground; however, in our case a *shallow* stable layer having a slightly elevated moisture content exists very close to the ground. The strongest downbursts may penetrate this stable layer, reaching the surface in the form of a heat burst. Weaker ones may only deform the stable layer.[5] The warming, drying and pressure falls that occur at the surface during heat bursts are consistent with this picture.

b. MCS dissipating stage and mesolow formation

By 0600 (Fig. 12a) the leading convective line has dissipated while the trailing stratiform rain area has expanded and strengthened. A strong mesohigh and diffluence center are centered in the stratiform region with two wake low centers to the rear. One hour later (Fig. 12b) these centers have drifted to the south, but the mesohigh is still centered in the stratiform area. Considerable dissipation of the stratiform rain area is evident by 0800 (Fig. 12c) with the mesohigh and wake low now shifting rapidly to the south.

A remarkable change in the surface pressure field occurs by 0900 (Fig. 12d). At this time the stratiform precipitation has nearly completely dissipated (also see Fig. 2e) and the region that was occupied only two hours earlier by a mesohigh now contains a pronounced mesolow having a central pressure approximately 5 mb lower than that of the surrounding environment on the south side. Two-hour pressure falls near the low center are as large as 7 mb. At 0900 there is only weak, if any, evidence of cyclonic turning of the surface wind around this mesolow. The flow indicates that the pressure changes have occurred too rapidly to permit adjustment to a balanced state (Garratt and Physick 1983).

This significant mesolow development occurs concurrently with the dissipation of the stratiform precipitation region. It is followed in 1 h by a weak cyclonic vortex cloud pattern as viewed by satellite (Fig. 2e), similar to those identified by Johnston (1982), Zhang and Fritsch (1988) and Menard and Fritsch (1988) following the decay of mesoscale convective systems. However, in addition to the suggestion of a midlevel vortex in the satellite data, here we see the rapid development of a pronounced surface low. Possibly similar mesolows were identified in the Johnstown, Pennsylvania, flood case by Bosart and Sanders (1981), and Zhang and Fritsch (1986). The scale of this feature in our case is sufficiently small that it would likely be very poorly detected or even completely undetected by conventional surface data.

The sequence of surface pressure analyses from 0600 to 0900 suggests that the strong mesolow at 0900 might be explainable as a southward propagation of the wake low. However, the propagation speed of the low center from 0800 to 0900, 28 m s^{-1}, seems excessive for this to be the case. Therefore, another formation mechanism appears to be operating. One candidate mechanism might be a collapsing cold pool, containing evaporating precipitation, initially characterized at the surface by a mesohigh. Later, following the removal of precipitation and adiabatic descent, lower tropospheric warming could occur and lead hydrostatically to a mesolow at the surface.

Surface observations indicate that, indeed, strong subsidence is occurring in the lower troposphere at the location of and at the time of the mesolow formation. A pronounced surface divergence center propagates to the south along with the mesohigh from 0200 to 0800. Values at 0600, the time of the strongest surface divergence, are shown in Fig. 13. The maximum value near the mesohigh center exceeds 3.5×10^{-4} s^{-1}. If averaged over a 500 m depth above the surface, this value corresponds to a downward motion at 500 m of about 20 cm s^{-1} (computation of vertical motion using sounding and Doppler radar data will be reported in Part II). Mesoscale subsidence this strong in the absence

[5] One such event occurring during OK PRE-STORM on 14 June was documented with Doppler radar data and was characterized by a spreading of the downburst atop the nocturnal inversion.

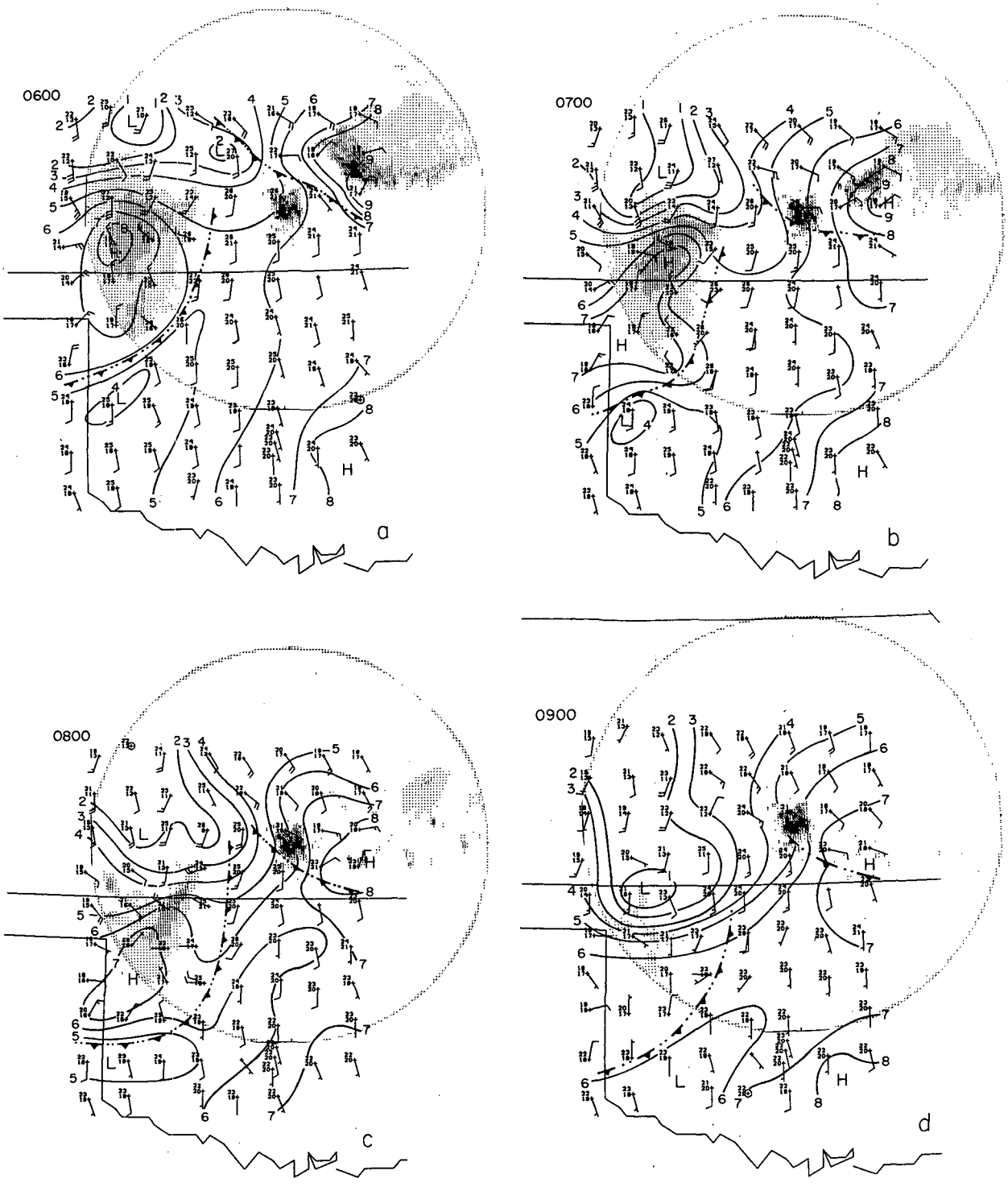

FIG. 12. Surface mesonetwork analyses as in Fig. 9, except at (a) 0600, (b) 0700, (c) 0800 and (d) 0900.

of precipitation could produce significant warming in a stably stratified atmosphere.

A realistic sounding upon which this subsidence is acting is that for Woodward (WWR), Oklahoma, at 0600, a sounding which was taken at the southern edge of the stratiform precipitation region (Fig. 14, dotted lines). Note that the lower troposphere is quite stable (nearly moist adiabatic) below 700 mb and that the sounding terminated just below 500 mb due to effects of the precipitation. By 0855, considerable warming

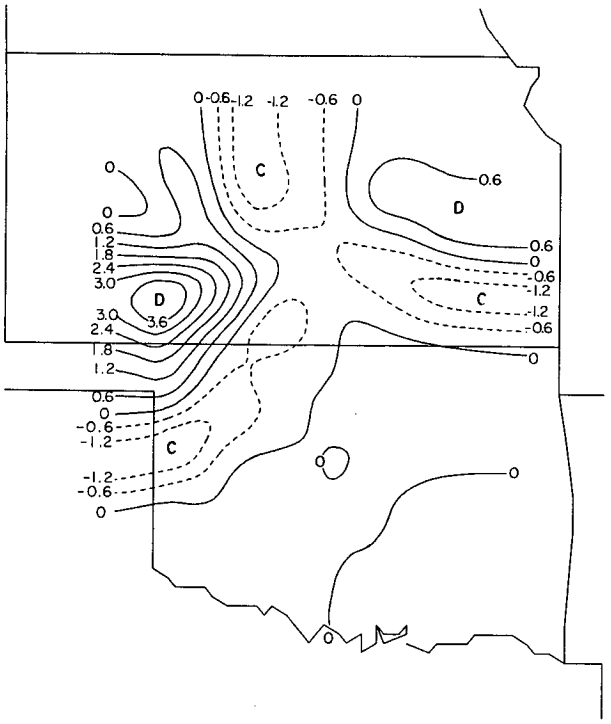

FIG. 13. Surface divergence (10^{-4} s^{-1}) at 0600 UTC 24 June 1985.

and drying has occurred at WWR (Fig. 14, solid lines). The mean virtual temperature change from the 0°C level (about 600 mb) to the surface is +4.1°C. Assuming the pressure in a column from 600 mb to the surface can be computed with reasonable accuracy using the mean virtual temperature $\bar{T}_v$ for the column, the surface hydrostatic pressure change associated with this warming is given by

$$\Delta P = 600[\exp(gz_f/R\bar{T}_{vf}) - \exp(gz_i/R\bar{T}_{vi})]$$
$$= -2.6 \text{ mb} \quad (2)$$

where z is the height above the ground of the 600 mb surface and i and f refer to initial (0600) and final (0855) values (z_i = 3763 m; z_f = 3793 m; $\bar{T}_{vi}$ = 286.3 K; $\bar{T}_{vf}$ = 290.4 K). This hydrostatic change is in reasonable agreement with the observed pressure change of −3.2 mb at WWR determined from the analyses in Figs. 12a and 12d. Just 50 km north of WWR, 3-h pressure falls up to 7 mb occurred, suggesting even stronger subsidence warming in that region. It is possible that some of the warming there is also occurring in the mid- to upper troposphere. If true, then the warm core analyzed at 500 mb in Fig. 5b may actually extend farther south than indicated. Several minor heat bursts occurred at P34 around 0900; however, they were not nearly as intense as those observed earlier due to the existence of a deeper surface inversion (Fig. 14), which apparently prevented the downdrafts from fully reaching the surface. From (1), it is estimated that a 12–15 m s^{-1} downdraft would be required to achieve penetration to the surface at this time.

These findings suggest that the rapid development of a surface mesolow following the decay of the 23–24 June MCS in OK PRE-STORM can be explained hydrostatically by lower-tropospheric subsidence warming in the dissipating stratiform region. Lower-tropospheric subsidence has also been identified as the mechanism producing wake lows in mature squall lines (Williams 1963; Johnson and Hamilton 1988); however, in those cases the surface low coexists with and occurs just to the rear of the stratiform precipitation region (as it did earlier in this case, Fig. 9).

The post-MCS surface mesolow, on the other hand, appears to develop directly beneath the stratiform cloud during its final decay. The rapid surface pressure falls from 0700 to 0900 (Fig. 12d) and coincident cessation of precipitation suggests that the dissipation of the stratiform region might be accurately characterized as a collapsing cold pool or spreading density current. We have conducted preliminary numerical modeling studies that indicate that indeed the rapid demise of the surface mesohigh and, to some extent, the development of the surface mesolow in its place can be explained by such a mechanism. This work is similar to the modeling studies of Miller and Betts (1977) and Thorpe et al. (1980). In all of these studies, warming was found to occur atop the spreading surface density

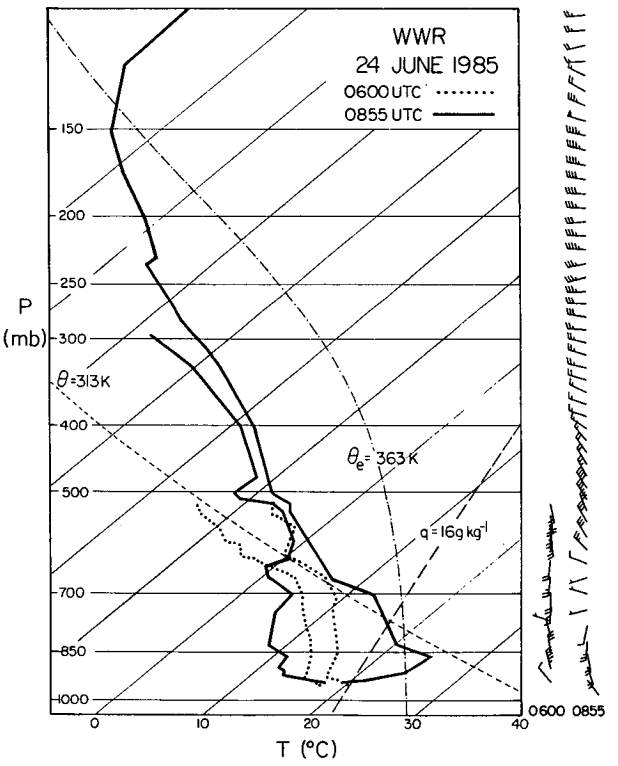

FIG. 14. Skew-T plots for Woodward, Oklahoma, at 0600 and 0855 UTC 24 June 1985.

current, hence accounting for the onion-type sounding structure often observed in such regions. While the outward spreading of cool air and subsidence warming in its place obviously leads to a reduction of surface pressure, the extent to which this process accounts for the rather intense low at 0900 (Fig. 12d) is not completely known. Other mechanisms for the pronounced surface mesolow development during the MCS decay may have existed, e.g., by warming aloft (Zhang and Fritsch 1986); however, we could not detect evidence of them. It appears in our case that the surface mesolow has a lower tropospheric origin and is separate and distinct from the midlevel cyclonic circulation evident at 500 mb.

c. *Decay of surface mesolow and development of new convection*

Over the next six hours the surface low drifted very slowly to the south and filled (Figs. 15a–c) with the surface flow remaining southerly throughout. By 1500 (early daytime; Fig. 15d) the low is gone with only a weak trough remaining; however, new convection has been triggered in southwest Kansas (Fig. 2f), presumably in association with the remnant midlevel mesovortex circulation. The slightly disturbed surface flow may also have contributed to the new development by creating localized surface convergence. As can be seen from Fig. 16, three PAM stations recorded rain from the redeveloped convective system (P19, P26, P27; see Fig. 15d for positions). At P19, 26 mm of rain fell from 1530 to 1700. Remarkably, this time series shows precipitation at the three stations from both the initial MCS and the subsequently generated system, separated by a period of about 12 h. Johnston (1982) and Menard and Fritsch (1988) showed examples of similar reintensification of MCSs in response to boundary layer heating, where, in some cases, the systems persisted for several days.

The mechanisms by which a decayed MCS can regenerate itself are not well known. However, the recent numerical modeling study by Crook et al. (1989) suggests that one possible mechanism is a mesoscale oscillation, whereby the warm region in a decayed MCS later rebounds or ascends (due to buoyancy) and resaturates the atmosphere. Unfortunately, we do not have the data to determine whether or not such a regeneration mechanism is working in our case.

6. Summary and conclusions

During the mature-to-decaying stages of a midlatitude mesoscale convective system (MCS) that occurred on 23–24 June 1985 over the OK PRE-STORM network, several dramatic surface phenomena were observed. The first was an episode of "heat bursts" (Johnson 1983) that persisted for approximately four hours at several mesonetwork stations situated just to the rear of the trailing stratiform region of the MCS during its mature stage. The second was a rapid transformation of a surface mesohigh to a mesolow (within 2 h), coincident with dissipation of the stratiform precipitation region and the development or intensification of a midtropospheric cyclonic circulation.

The MCS under study was the westernmost of two that developed over the central United States on the afternoon of 23 June. The initial convective cells formed along a dryline in western Kansas. The cells later merged into an arc-shaped, east–west band of convection that propagated to the south at about 10 m s^{-1} in an environment of weak vertical wind shear. During its growing and mature stages (spanning the evening and late night hours), the convective line developed a trailing stratiform precipitation region to its north having a ~200 km horizontal dimension.

As the stratiform precipitation region expanded, a surface wake low appeared along its northern edge, and within this region the heat bursts occurred. Our analysis supports the hypothesis of Johnson (1983) that heat bursts are essentially downbursts (Fujita 1985) initiated from the trailing stratiform cloud which penetrate through a shallow stable layer near the ground. We do not have direct measurements of the downbursts since the heat burst area was at the limiting range of the NCAR CP-3 Doppler radar; however, there is confirmation from the radar data of a relatively deep stratiform cloud above the heat burst site. The shallow stable layer in the region is produced by outflows from the leading convective line (Zipser 1977). The mesoscale downdraft beneath and slightly to the rear of the trailing stratiform cloud produces the deep, nearly dry-adiabatic layer that is conducive to strong localized downdrafts. These conditions favorable for heat bursts require a unique combination of events, in contrast with the more commonly observed High Plains microbursts which occur in nearly dry-adiabatic layers extending to the surface. This unique environmental structure is a special case of the typical "onion" sounding structure occurring to the rear of trailing stratiform cloud systems (Zipser 1977). In most reported instances of the onion sounding structure, a relatively deep stable layer exists near the ground as a result of the spreading of very cool air from convective downdrafts. In such cases, downbursts do not appear to be able to penetrate to the surface (Zipser 1977). In the heat burst case, this stable layer is very shallow and the downbursts can reach the ground. What makes the heat burst environment a rare event is not entirely clear; however, perhaps such a situation is favored when mesoscale convective systems develop in relatively hot, dry conditions as observed on this day and also reported in the heat burst case studied by Johnson (1983).

While the stratiform precipitation region persisted, an intense mesohigh was observed at the surface beneath it. In a relatively short time (2–3 h) the stratiform precipitation dissipated and the surface mesohigh

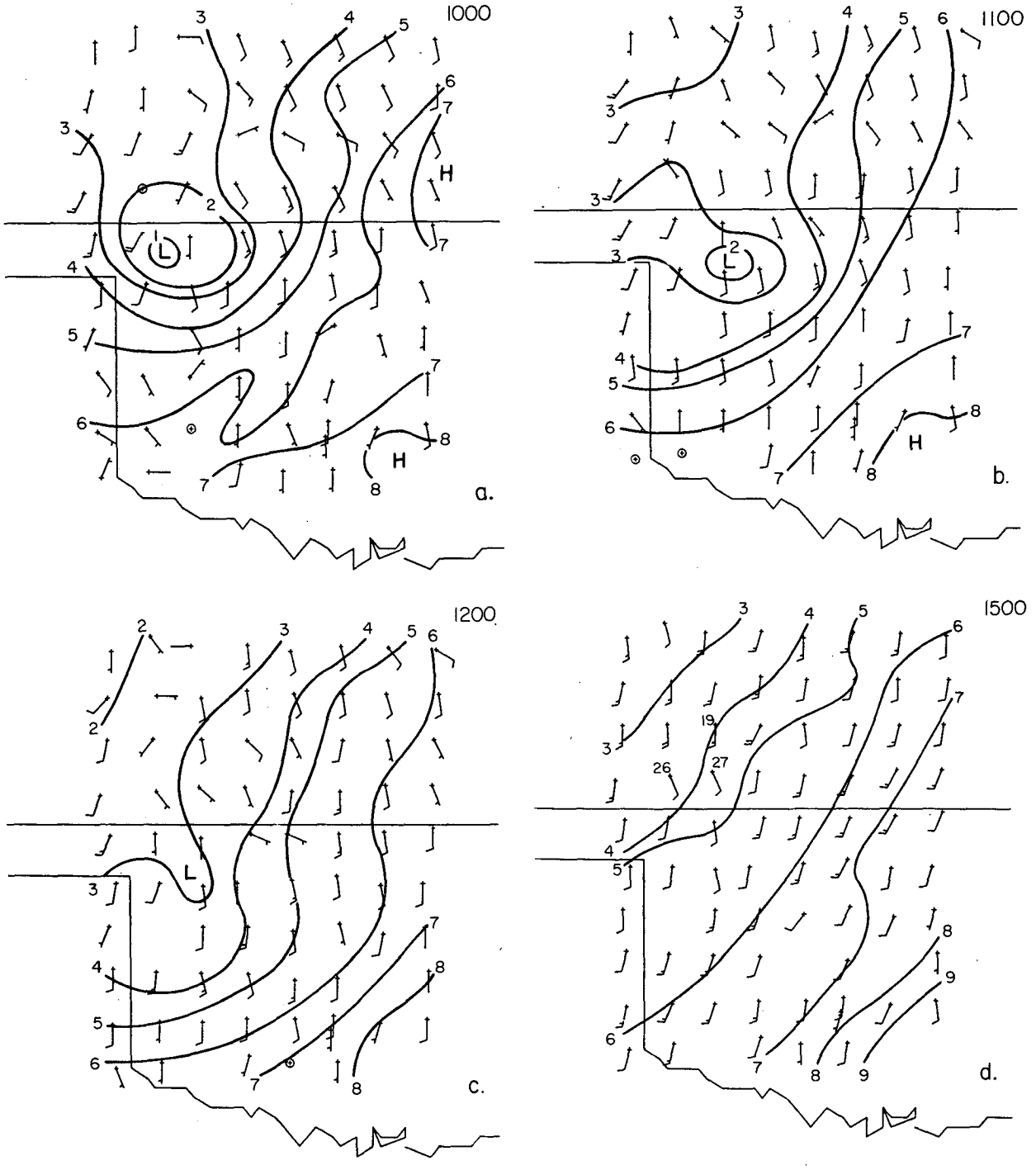

FIG. 15. Surface mesonetwork analyses as in Fig. 9, except for (a) 1000, (b) 1100, (c) 1200 and (d) 1500.

transformed to a mesolow. Analysis of sounding data suggests that the development of the mesolow can be explained reasonably well hydrostatically in terms of lower tropospheric subsidence warming. The outward spreading of the surface cold pool following the collapse of the stratiform region may have accounted for the strong, rapid warming. A preliminary numerical modeling study that we have conducted and the works of Miller and Betts (1977) and Thorpe et al. (1980) support this idea.

Sounding observations show the development or intensification of a midtropospheric mesovortex on the

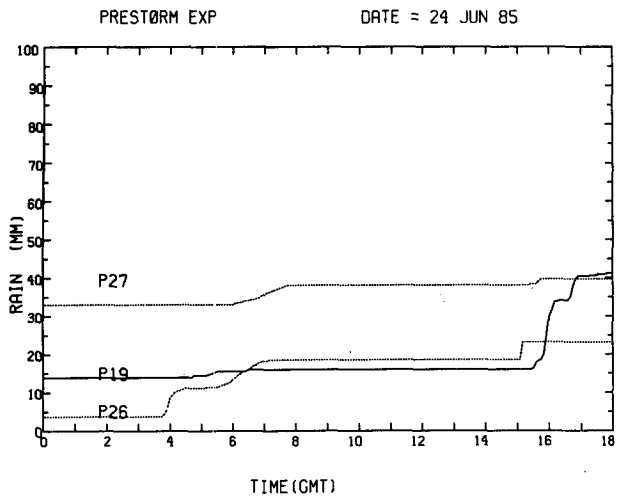

FIG. 16. Time series of accumulated rainfall (mm) at PAM stations 19, 26 and 27 (see Fig. 15d for positions) from 0000 to 1800 UTC 24 June 1985.

morning of 24 June with evidence of cyclonically spiralling midlevel clouds in the satellite data. This mesovortex feature is of the same character as those reported in the studies of Johnston (1982), Zhang and Fritsch (1987, 1988), Velasco and Fritsch (1987) and Menard and Fritsch (1988). It is apparent from the observations of strong surface divergence throughout the ~6 h lifetime of this precipitation feature that the circulation may have been a consequence of prolonged midtropospheric inflow compensating the low-level outflow. This vertical stretching in the midtroposphere occurred in a large-scale environment characterized by large positive vorticity initially (as a shear line appeared to enter the region from the north), which may have assisted in the spinup. Details of the upper-level structure of the mesovortex will be reported in Part II.

After sunrise on 24 June, a redevelopment of deep convection occurred (as in Menard and Fritsch 1988). The surface mesolow persisted until about the time of this redevelopment and may have played some role in the initiation of new deep convection. However, other processes may have occurred [such as a mesoscale oscillation set up by the previous squall system (Crook et al. 1989)] and this aspect of these phenomena deserves further study.

Acknowledgments. This paper has benefited greatly from comments by Bob Maddox and Ed Zipser. The use of the CSU Regional Atmospheric Modeling System, under the direction of Bill Cotton, for conducting several preliminary modeling studies is gratefully acknowledged. Discussions with Mel Nicholls and Peggy LeMone were also helpful. Our appreciation is also extended to José Meitín, Dave Jorgensen and Irv Watson of NOAA and Jim Bresch of CSU for their assistance in data acquisition, analysis and modeling efforts. We thank Gail Cordova for preparing the manuscript. Computing resources were obtained, in part, from the Scientific Computing Division, National Center for Atmospheric Research. This research has been supported by the National Science Foundation, Atmospheric Sciences Division, under Grants ATM-8507961 and ATM-8711649.

REFERENCES

Augustine, J. A., and E. J. Zipser, 1987: The use of wind profilers in a mesoscale experiment. *Bull. Amer. Meteor. Soc.*, **68**, 4–17.

Bedard, A. J., Jr., and T. T. LeFebvre, 1986: Surface measurements of gust fronts and microbursts during the JAWS Project: Statistical results and implications for wind shear detection, prediction and modeling. NOAA Tech. Memo. ERL WPL-135, 112 pp. [NTIS PB86-200847.]

Bosart, L. R., and F. Sanders, 1981: The Johnstown flood of July 1977: A long-lived convective storm. *J. Atmos. Sci.*, **38**, 1616–1642.

Brown, J. M., 1979: Mesoscale unsaturated downdrafts driven by rainfall evaporation: A numerical study. *J. Atmos. Sci.*, **36**, 313–338.

——, K. R. Knupp and F. Caracena, 1982: Destructive winds from shallow, high-based cumulonimbi. Preprints, *12th Conference on Severe Local Storms*, San Antonio, Amer. Meteor. Soc., 272–275.

Cheng, C.-P., and R. A. Houze, Jr., 1979: The distribution of convective and mesoscale precipitation in GATE radar echo patterns. *Mon. Wea. Rev.*, **107**, 1370–1381.

Chong, M., P. Amayenc, G. Scialom and J. Testud, 1987: A tropical squall line observed during the COPT 81 experiment in West Africa. Part 1: Kinematic structure inferred from dual-Doppler radar data. *Mon. Wea. Rev.*, **115**, 670–694.

Churchill, D. D., and R. A. Houze, Jr., 1984: Development and structure of winter monsoon cloud clusters on 10 December 1978. *J. Atmos. Sci.*, **41**, 933–960.

Crook, N. A., R. E. Carbone, M. W. Moncrieff and J. W. Conway, 1989. The generation and propagation of a nocturnal squall line. Part II: Numerical simulations. *Mon. Wea. Rev.*, **117**, submitted.

Cunning, J. B., 1986: The Oklahoma–Kansas Preliminary Regional Experiment for STORM-Central. *Bull. Amer. Meteor. Soc.*, **67**, 1478–1486.

Fritsch, J. M., and C. G. Chappell, 1980: Numerical prediction of convectively driven mesoscale pressure systems. Part II: Mesoscale model. *J. Atmos. Sci.*, **37**, 1734–1762.

——, and R. A. Maddox, 1981a: Convectively driven mesoscale pressure systems aloft. Part I: Observations. *J. Appl. Meteor.*, **20**, 9–19.

——, and ——, 1981b: Convectively driven mesoscale pressure systems aloft. Part II: Numerical simulations. *J. Appl. Meteor.*, **20**, 20–26.

Fujita, T. T., 1955: Results of detailed synoptic studies of squall lines. *Tellus*, **7**, 405–436.

——, 1985: The Downburst. SMRP Research Paper Number 210, Dept. of Geophysical Sciences, University of Chicago, 122 pp. [NTIS PB-148880.]

——, and R. M. Wakimoto, 1981: Five scales of airflow associated with a series of downbursts on 16 July 1980. *Mon. Wea. Rev.*, **109**, 1438–1456.

Gamache, J. F., and R. A. Houze, Jr., 1982: Mesoscale air motions associated with a tropical squall line. *Mon. Wea. Rev.*, **110**, 118–135.

Garratt, J., and W. L. Physick, 1983: Low-level wind response to mesoscale pressure systems. *Bound.-Layer Meteor.*, **27**, 69–87.

Houze, R. A., Jr., 1977: Structure and dynamics of a tropical squall-line system. *Mon. Wea. Rev.*, **105**, 1540–1567.

——, and P. V. Hobbs, 1982: Organization and structure of precipitating cloud systems. *Advances in Geophysics*, Vol. 24, Academic Press, 225–315.

——, and E. N. Rappaport, 1984: Air motions and precipitation structure of an early summer squall line over the eastern tropical Atlantic. *J. Atmos. Sci.*, **41**, 553–574.

Johnson, B. C., 1983: The heat burst of 29 May 1976. *Mon. Wea. Rev.*, **111,** 1776–1792.

Johnson, R. H., and P. J. Hamilton, 1988: The relationship of surface pressure features to the precipitation and air flow structure of an intense midlatitude squall line. *Mon. Wea. Rev.*, **116,** 1444–1472.

Johnston, E. C., 1982: Mesoscale vorticity centers induced by mesoscale convective complexes. Preprints, *Ninth Conference on Weather Forecasting and Analysis,* Seattle, Amer. Meteor. Soc., 196–200.

Leary, C. A., 1979: Behavior of the wind field in the vicinity of a cloud cluster in the intertropical convergence zone. *J. Atmos. Sci.*, **36,** 631–639.

——, 1984: Precipitation structure of the cloud clusters in a tropical easterly wave. *Mon. Wea. Rev.*, **112,** 313–325.

——, and E. N. Rappaport, 1987: The life cycle and internal structure of a mesoscale convective complex. *Mon. Wea. Rev.*, **115,** 1503–1527.

Maddox, R. A., 1983: Large-scale meteorological conditions associated with midlatitude, mesoscale convective complexes. *Mon. Wea. Rev.*, **111,** 1475–1493.

——, D. J. Perkey and J. M. Fritsch, 1981: Evolution of upper tropospheric features during the development of a mesoscale convective complex. *J. Atmos. Sci.*, **38,** 1664–1674.

Menard, R. D., and J. M. Fritsch, 1989: An MCC-generated inertially stable warm core vortex. *Mon. Wea. Rev.*, **117,** 1237–1261.

Miller, M. J., and A. K. Betts, 1977: Traveling convective storms over Venezuela. *Mon. Wea. Rev.*, **105,** 833–848.

Ogura, Y., and M. T. Liou, 1980: The structure of a mid-latitude squall line: A case study. *J. Atmos. Sci.*, **37,** 553–567.

Pedgley, D. E., 1962: A meso-synoptic analysis of the thunderstorms on 28 August 1958. Brit. Meteor. Off., Geophys. Mem., No. 106, 74 pp.

Rutledge, S. A., and R. A. Houze, Jr., 1987: A diagnostic modeling study of the trailing stratiform region of a midlatitude squall line. *J. Atmos. Sci.*, **44,** 2640–2656.

——, ——, M. I. Biggerstaff and T. Matejka, 1988: The Oklahoma–Kansas mesoscale convective system of 10–11 June 1985: Precipitation structure and single-Doppler radar analysis. *Mon. Wea. Rev.*, **116,** 1409–1430.

Sangster, W. E., 1987: An improved technique for computing the horizontal pressure-gradient force at the earth's surface. *Mon. Wea. Rev.*, **115,** 1358–1369.

Smull, B. F., and R. A. Houze, Jr., 1985: A midlatitude squall line with a trailing region of stratiform rain: Radar and satellite observations. *Mon. Wea. Rev.*, **113,** 117–133.

——, and ——, 1987a: Dual-Doppler radar analysis of a mid-latitude squall line with a trailing region of stratiform rain. *J. Atmos. Sci.*, **44,** 2128–2148.

——, and ——, 1987b: Rear inflow in squall lines with trailing stratiform precipitation. *Mon. Wea. Rev.*, **115,** 2869–2889.

Stensrud, D. J., and R. A. Maddox, 1988: Opposing mesoscale circulations: A case study. *Wea. Forecasting,* **3,** 189–204.

Thorpe, A. J., M. J. Miller and M. W. Moncrieff, 1980: Dynamical models of two-dimensional downdraughts. *Quart. J. Roy. Meteor. Soc.*, **106,** 463–484.

Velasco, I., and J. M. Fritsch, 1987: Mesoscale convective complexes in the Americas. *J. Geophys. Res.*, **92,** 9591–9613.

Wakimoto, R. M., 1985: Forecasting dry microburst activity over the High Plains. *Mon. Wea. Rev.*, **113,** 1131–1143.

Wei, T., and R. A. Houze, Jr., 1987: The GATE squall line of 9–10 August 1974. *Advances in Atmospheric Sciences,* Vol. 4, 85–92.

Wetzel, P. J., W. R. Cotton and R. L. McAnelly, 1983: A long-lived mesoscale convective complex. Part II: Evolution and structure of the mature complex. *Mon. Wea. Rev.*, **111,** 1919–1937.

Williams, D. T., 1963: The thunderstorm wake of May 4, 1961. Natl. Severe Storms Project Rep. No. 18, U.S. Dept. of Commerce, Washington, D.C., 23 pp. [NTIS PB 168223.]

Zhang, D.-L., and J. M. Fritsch, 1986: Numerical simulation of the meso-β scale structure and evolution of the 1977 Johnstown flood. Part I: Model description and verification. *J. Atmos. Sci.*, **43,** 1913–1943.

——, and ——, 1987: Numerical simulation of the meso-β scale structure and evolution of the 1977 Johnstown flood. Part II: Inertially stable warm-core vortex and the mesoscale convective complex. *J. Atmos. Sci.*, **44,** 2593–2612.

——, and ——, 1988: A numerical investigation of a convectively generated, inertially stable, extratropical warm-core mesovortex over land. Part I: Structure and evolution. *Mon. Wea. Rev.*, **116,** 2660–2687.

Zipser, E. J., 1977: Mesoscale and convective-scale downdrafts as distinct components of squall-line circulation. *Mon. Wea. Rev.*, **105,** 1568–1589.